© Pol J Radiol 2026; 91: e478-e483
DOI: https://doi.org/10.5114/pjr/219937

Received: 22.01.2026
Accepted: 24.03.2026
Published: 05.10.2026

Polish Journal of Radiology

http://www.polradiol.com

Original paper

Morphometric and tortuosity analysis of internal carotid artery harbouring small and large aneurysms: a comprehensive quantitative study

Maciej Jakub Frączek[1,2,A,D,E,F], Roger Marek Krzyżewski[1,A,B,C,D], Kornelia Maria Kliś[1,A,B,C,D,E], Borys Maria Kwinta[1,A,E], Tadeusz Popiela[3,A,B], Krzysztof Stachura[1,A,E]

[1]Department of Neurosurgery and Neurotraumatology, Faculty of Medicine, Jagiellonian University Medical College, Krakow, Poland
[2]Doctoral School of Medical and Health Sciences, Jagiellonian University Medical College, Krakow, Poland
[3]Chair of Radiology, Faculty of Medicine, Jagiellonian University Medical College, Krakow, Poland

Abstract

Purpose: Intracranial aneurysms display diverse morphologies influenced by parent vessel geometry. The role of 3D vessel tortuosity in differentiating small from large aneurysms remains underexplored. The aim of this study was to comprehensively analyse morphometric and tortuosity parameters of internal carotid arteries (ICAs) harbouring small (< 5 mm) versus large (≥ 5 mm) aneurysms using advanced 3D imaging.

Material and methods: This retrospective study included 48 patients with unruptured unilateral ICA aneurysms (21 small, 27 large) without previous interventions. 3D digital subtraction angiography imaging was used to reconstruct arterial models. We extracted morphometric parameters (radius, length) and tortuosity metrics including relative length (RL), sum-of-angle metric (SOAM), inflection count metric (ICM), and normalised curvature/torsion using validated algorithms.

Results: The ICA radius was significantly smaller in the small-aneurysm group (2.08 ±0.27 mm vs. 2.22 ±0.17 mm; $p = 0.039$). Vessels with small aneurysms demonstrated higher tortuosity: normalised torsion (3.89 ± 6.96 vs. –3.43 ± 9.96; $p = 0.005$), normalised curvature (8.91 ± 4.14 vs. 5.56 ± 5.75; $p = 0.025$), lower RL (0.56 ± 0.08 vs. 0.63 ± 0.05; $p = 0.002$), higher SOAM (2.48 ± 0.56 vs. 2.14 ± 0.51; $p = 0.034$), and elevated ICM (8.54 ± 3.07 vs. 5.95 ± 2.60; $p = 0.004$).

Conclusions: Small ICA aneurysms occur preferentially on more tortuous vessels with a smaller parent-artery radius. These findings support the integration of 3D vessel geometry metrics into research of aneurysm risk stratification and treatment planning algorithms.

Key words: neurosurgery, subarachnoid haemorrhage, intracranial aneurysm, angiography.

Introduction

Intracranial aneurysms (IAs) are pathological dilations of cerebral arteries that pose a significant risk of rupture, leading to subarachnoid haemorrhage and high morbidity and mortality. The assessment of aneurysm rupture risk remains a critical challenge in neurovascular medicine because clinical decision-making relies on the accurate evaluation of both morphological and haemodynamic factors [1].

Various research suggests that the majority of all IAs are rather small (< 7 mm) [2-4], with some findings suggesting that they can account for over 90% of all IA cases [5].

Correspondence address:
Maciej Jakub Frączek, Department of Neurosurgery and Neurotraumatology, Faculty of Medicine, Jagiellonian University Medical College, 2 Jakubowskiego St., 30-688 Krakow, Poland, e-mail: f.maciej21@gmail.com

Authors' contribution:
A Study design · **B** Data collection · **C** Statistical analysis · **D** Data interpretation · **E** Manuscript preparation · **F** Literature search · **G** Funds collection

This is an Open Access journal, all articles are distributed under the terms of the Creative Commons Attribution-Noncommercial-No Derivatives 4.0 International (CC BY-NC-ND 4.0). License (https://creativecommons.org/licenses/by-nc-nd/4.0/).

Current decision-making is often guided by aneurysm size, location, and patient-related risk factors summarised in scoring systems such as population, hypertension, age, size of aneurysm, earlier subarachnoid hemorrhage (PHASES) [6] or Unruptured Intracranial Aneurysm Treatment Score (UIATS) [7]. However, these frameworks have limited predictive accuracy, as many small aneurysms rupture while some larger ones remain stable over a lifetime. Aneurysm and parent vessel morphology analysis is one of the novel features that can elevate rupture prediction precision. Traditional parameters such as dome size, neck width, aspect ratio, dome-to-neck ratio, and size ratio are routinely measured to estimate rupture risk [1,8,9].

Computational fluid dynamics (CFD) simulations have become integral to understanding the haemodynamic environment within aneurysms, allowing quantification of wall shear stress, oscillatory shear index, and complex flow patterns that have been implicated in aneurysm growth and rupture. Although the predictive value of individual haemodynamic parameters remains under investigation, prior work combining CFD with morphological descriptors has demonstrated improved risk stratification [8,9].

Additionally, the tortuosity of cerebral arteries – quantified through geometric and curvature-based indices – has been recognised as a marker of vascular disease burden and may influence local haemodynamics and aneurysm formation. However, due to the complex nature of vessel geometry, especially that of the internal carotid artery (ICA), it remains challenging to comprehensively describe its tortuosity. Many descriptors have been proposed, and the role of each in the aneurysm formation or development process remains inconclusive. The current development of robust, automated pipelines for tortuosity measurement further supports comprehensive evaluation of cerebrovascular pathology [10-12].

Therefore, the present study aimed to systematically analyse tortuosity parameters of ICAs harbouring small (< 5 mm) versus larger (≥ 5 mm) aneurysms. Using advanced 3D angiographic reconstructions, we sought to determine whether vessel tortuosity provide additional discriminatory value beyond traditional size-based assessment. We hypothesised that arteries bearing small aneurysms would demonstrate greater tortuosity and geometric complexity, potentially reflecting distinct mechanistic pathways in aneurysm pathophysiology.

Material and methods

This retrospective study utilised data from the medical records of patients hospitalised at the Department of Neurosurgery and Neurotraumatology, Jagiellonian University Medical College in Cracow, Poland, for unruptured IAs of the ICA.

This study was intentionally restricted to unruptured unilateral ICA aneurysms to minimise anatomical heterogeneity and reduce confounding due to location-dependent flow patterns.

Exclusion criteria comprised the presence of any other intracranial pathologies, previous neurosurgical or endovascular interventions, and history of ischaemic stroke or subarachnoid haemorrhage.

Data were collected from electronic medical records by the authors of this study. The collected data included basic demographic characteristics, such as age, sex, medical history, and imaging data. Aneurysms were categorised as small or large, according to dome size. Threshold was set at 5 mm in maximal dome size measured. A cutoff value was chosen as we aimed to capture subtle geometric differences in parent-artery tortuosity that may already be present in very small lesions. While a 7-mm threshold is frequently used to dichotomise aneurysm size in rupture-risk studies, our focus was on geometry across the small-to-moderate size spectrum rather than on direct rupture risk stratification.

Vessel morphology and tortuosity analysis

All morphological analyses were performed on digital subtraction angiography (DSA) studies acquired as part of the standard diagnostic work-up before any endovascular intervention was undertaken. Inclusion was based solely on baseline imaging and clinical data, irrespective of whether patients ultimately underwent treatment or conservative management. All assessments were taken only on the unilateral ICA harbouring an IA. The neuroradiology specialist performed aneurysm dome measurements.

For all prepared ICA models, we extracted its centrelines (from the point of its origin to the point of its bifurcation) using Vascular Modeling Toolkit 1.4 [13]. Using our own software, written in Python 3.9 with NumPy and Visualization Toolkit libraries, we further analysed the centrelines' tortuosity. For patient-specific models we extracted the number of angles, measures, and arc lengths. Then, we extracted the following tortuosity parameters of all models, which are presented in Figure 1:

- relative length (RL), sum-of-angle metric (SOAM), triangular index (TI), and inflection-count metric (ICM) [12,14];
- curvature (κ) measured in each point on a line $c(s)$ parametrised through curvilinear abscissa, defined as:

$$\kappa(s) = \frac{|c'(s) \times c''(s)|}{|c'(s)|^3}$$

- torsion (τ) measured in each point on a line $c(s)$ parametrised through curvilinear abscissa, defined as:

$$\tau = \frac{[c'(s) \times c''(s)] \cdot c'''(s)}{[c'(s) \times c(s)]}$$

- curvature normalised to length (c_n) defined as:

$$\kappa_n = \frac{\int_0^L \kappa(s) ds}{L}$$

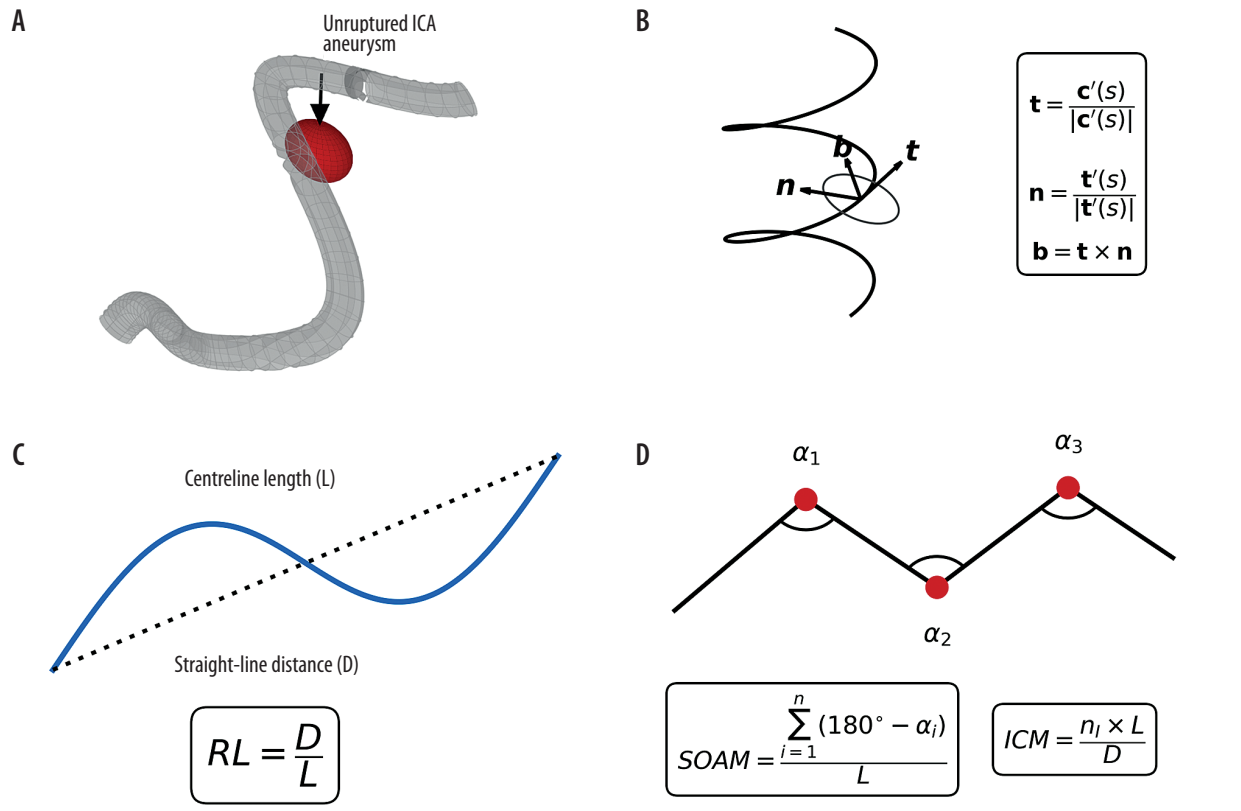


Figure 1. A) Schematic 3D reconstruction of the internal carotid artery (ICA) harbouring an unruptured aneurysm (arrow). The model illustrates the vascular geometry used for centreline extraction. **B**) Visualisation of the Frenet-Serret coordinate system along a helical curve segment. The moving frame consists of three orthogonal unit vectors: the tangent (t), normal (n), and binormal (b). The normal plane (ellipse) is orthogonal to the tangent vector t. **C**) Definition of the relative length (RL) metric, calculated as the ratio between the straight-line Euclidean distance (D) between the vessel origin and bifurcation and the actual centreline length (L). **D**) Schematic representation of angle-based tortuosity metrics calculated from the centreline. The sum-of-angle metric (SOAM) is defined as the sum of supplementary angles normalised by the centreline length. The inflection count metric (ICM) is calculated as the number of inflection points multiplied by the centreline length and divided by the Euclidean distance

where L is the curve length and $\kappa(s)$ are curvature values in curve points;

- torsion normalised to length (τ_n), defined as:

$$\tau_n = \frac{\int_0^L \tau(s)ds}{L}$$

where L is the curve length and $\tau(s)$ are curvature values in curve points;

- curvature normalised to distance (κ_d) defined as:

$$\kappa_d = \int_0^L \frac{\kappa(s)}{d(s)} ds$$

where $d(s)$ is the distance of point – where $\kappa(s)$ was measured – to bifurcation;

- distance-tortuosity index (DTI):

$$DTI = \sum_{n=1}^{N} \frac{\alpha_n}{\Sigma_{i=1}^{n} l_i}$$

where N is the number of angles on the artery course, α_n is the angle measure, and l_i is the arc length (with α_1 and l_1 representing arc and angle closest to bifurcation).

Results

The cohort included 48 single, ICA aneurysms (21 small, 27 large). Population characteristics are available in Table 1 and Table 2. No significant differences were observed in age (56.5 ± 12.59 vs. 58.0 ± 14.75 years; $p = 0.71$), sex distribution (71.4% vs. 77.8% female; $p = 0.70$), or cardiovascular risk factors between small and large aneurysm cohorts (all $p > 0.05$). As expected, aneurysm dome size was significantly smaller in the small-aneurysm group than in the large-aneurysm group (3.41 ± 0.91 mm vs. 7.50 ± 3.11 mm; $p < 0.001$). Morphometric analysis revealed that the parent ICA radius was significantly smaller in the small-aneurysm group (2.08 ± 0.27 mm vs. 2.22 ± 0.17 mm; $p = 0.039$). Tortuosity metrics differed markedly: torsion and curvature normalised to artery length was higher in vessels with small aneurysms (mean 3.89 vs. −3.43; $p = 0.005$), as was normalised curvature (8.91 vs. 5.56; $p = 0.025$). RL was significantly lower in the small-aneurysm group (0.56 vs. 0.63; $p = 0.002$), indicating greater overall vessel tortuosity. Similarly, SOAM was higher

Table 1. Demographic and clinical characteristics of the study cohort ($N = 48$)

Variable	
Age (years), mean ± SD	57.17 ± 13.69
Female gender, *n* (%)	36 (75.00)
Aneurysm dome size (mm)	5.67 ± 3.14
Aneurysm neck size (mm)	3.99 ± 1.46
Small aneurysms, *n* (%)	21 (43.75)
Right side, *n* (%)	27 (56.25)
Comorbidities, *n* (%)	
Hypertension	25 (52.08)
Diabetes	6 (12.50)
Smoking	5 (10.42)
Dyslipidaemia	2 (4.17)

in the small-aneurysm group (2.48 vs. 2.14; $p = 0.034$), and the ICM was elevated (8.54 vs. 5.95; $p = 0.004$). These findings indicate that ICA harbouring small (< 5 mm) aneurysms were more tortuous than those with larger aneurysms. In contrast, other vessel descriptors showed no significant group differences (all $p > 0.05$). In summary, the small-aneurysm group was characterised by significantly smaller parent-vessel radius and higher vessel tortuosity (RL, normalised torsion/curvature, SOAM, ICM) than the large-aneurysm group, while standard flow metrics were similar (Table 3, Figure 2).

Discussion

This study found that small IAs of ICA occur on more tortuous parent vessels than large aneurysms, together with a smaller parent artery radius. The significantly higher normalised curvature and torsion in the small-aneurysm group, along with lower RL and higher SOAM/ICM (all $p < 0.05$), indicate that vessels bearing small aneurysms have more frequent bends and inflections. These results suggest a strong coupling between parent-vessel geometry and aneurysm size.

Prior reports have also linked vessel tortuosity to aneurysm formation. Kim *et al.* [11] reported that higher TIs of intracranial arteries are associated with the occurrence of aneurysms. Similarly, Li *et al.* [15] found that arterial tortuosity correlates with aneurysm occurrence, while paradoxically inversely correlating with enlargement/rupture risk. In other words, tortuous arteries tend to develop aneurysms, but greater tortuosity appears protective against aneurysm growth or rupture [15]. This is inconsistent with Krzyżewski *et al.* [8], who noted that higher ICA tortuosity was linked to aneurysm growth. In contrast, our current findings indicate that patients with larger aneurysms exhibit lower ICA tortuosity. This apparent discrepancy may stem from methodological differences: our previous study relied on 2D analysis of DSA images, which may over- or underestimate vessel curvature due to projection artifacts and lack of spatial resolution. In the present work, we employed a 3D approach with centreline extraction from volumetric reconstructions, allowing more precise quantification of vascular geometry. Therefore, the current results probably provide a more accurate representation of the relationship between ICA tortuosity and aneurysm size, suggesting that lower tortuosity may facilitate aneurysm expansion, or that aneurysm growth may itself alter local vessel geometry.

Based on previous research, aneurysms – especially small ones – may preferentially form on curvy vessel segments, whereas straighter vessels could permit aneurysms to expand or rupture more easily [12]. Our analysis of curvature and torsion can be viewed in the same vein: subtle geometric descriptors (normalised curvature/torsion, tortuosity descriptors) capture differences that aneurysm diameter alone does not. Furthermore, Benemerito *et al.* [16] showed that augmenting the PHASES clinical score with image-derived shape and CFD features significantly improved aneurysm rupture classification, with the area

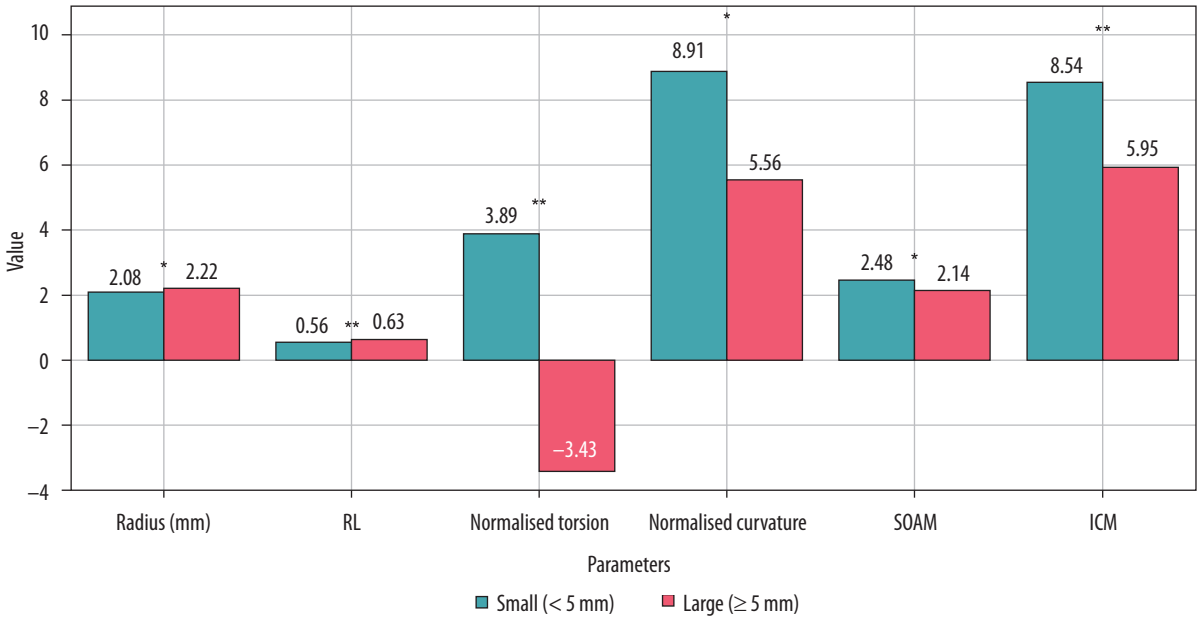
Table 2. Comparison of demographic and clinical variables between patients with small (< 5 mm) and large (≥ 5 mm) intracranial aneurysms

Variable	Small aneurysm ($n = 21$)	Large aneurysm ($n = 27$)	*p*-value
Age (years), mean ± SD	56.5 ± 12.59	58.0 ± 14.75	0.71
Female gender, *n* (%)	15 (71.42)	21 (77.77)	0.70
Right side, *n* (%)	13 (61.90)	14 (51.85)	0.53
Dome size [mm]	3.41 ± 0.91	7.5 ± 3.11	< 0.001
Comorbidities, *n* (%)			
Hypertension	12 (57.14)	13 (48.14)	0.63
Diabetes	1 (4.76)	5 (18.51)	0.14
Smoking	1 (4.76)	4 (14.81)	0.09
Dyslipidaemia	0 (0)	2 (7.40)	0.19

Table 3. Comparison of tortuosity and morphometric data between small and large cerebral aneurysms

Variable	Small aneurysm ($n = 21$)	Large aneurysm ($n = 27$)	p-value
Length	75.69 ± 10.5	75.84 ± 8.52	0.961
Sum torsion	–8.77 ± 61.68	–37.08 ± 67.97	0.142
Mean torsion	–0.03 ± 0.08	–0.04 ± 0.08	0.457
Sum curvature	115.72 ± 70.41	106.86 ± 57.3	0.644
Mean curvature	0.15 ± 0.02	0.14 ± 0.02	0.135
Radius	2.08 ± 0.27	2.22 ± 0.17	0.039
Torsion normalised to length	3.89 ± 6.96	–3.43 ± 9.96	0.005
Curvature normalised to length	8.91 ± 4.14	5.56 ± 5.75	0.025
RL	0.56 ± 0.08	0.63 ± 0.05	0.002
Mean angle	110.22 ± 13.26	116.74 ± 10.95	0.077
Mean arc	13.09 ± 2.76	13.9 ± 3.22	0.362
SOAM	2.48 ± 0.56	2.14 ± 0.51	0.034
TI	1.31 ± 0.15	1.24 ± 0.14	0.142
ICM	8.54 ± 3.07	5.95 ± 2.6	0.004
Mean arc angle	4.46 ± 1.57	4.39 ± 1.82	0.881
Angle arc distance	0.18 ± 0.11	0.16 ± 0.14	0.625
DTI	15.62 ± 11.57	14.8 ± 11.56	0.81

DTI – distance-tortuosity index, ICM – inflection count metric, RL – relative length, SOAM – sum-of-angle metric, TI – triangular index



*$p < 0.05$, **$p < 0.01$
ICM – inflection count metric, RL – relative length, SOAM – sum-of-angle metric

Figure 2. Comparison of morphometric and tortuosity parameters between small and large internal carotid artery aneurysms. Small aneurysms occur on more tortuous vessels with smaller parent artery radius. Data presented as mean values for $n = 21$ small aneurysms (< 5 mm) and $n = 27$ large aneurysms (≥ 5 mm)

under the receiver operating characteristic curve increasing from 0.63 to 0.71.

Clinically, the observed geometry–aneurysm relationship has potential implications. We can hypothesise that small aneurysms on tortuous vessels may harbour different rupture risk profiles than those on straighter arteries. Due to the retrospective nature of this study, we cannot assess how the observed correlations affect rupture risk. At present, tortuosity metrics should be regarded as hypothesis-generating imaging markers rather than decision-making tools. Incorporating quantitative vessel-shape descriptors into future multivari-

able prediction models may improve individualised risk stratification, but this concept requires prospective validation before any change in clinical practice can be recommended.

Moreover, knowledge of parent-artery tortuosity is relevant for endovascular planning: highly curved access vessels can complicate catheter navigation and may influence device selection. Overall, our data support the addition of quantitative vessel-shape descriptors to existing guidelines like PHASES or UIATS, aligning with the trend of image-based risk models [10,16].

This study has several limitations. First, the sample size was modest (48 aneurysms) and derived from a single tertiary centre, which limits statistical power and external validity. Second, we focused exclusively on ICA aneurysms, so the observed associations between vessel tortuosity and aneurysm size may not apply to aneurysms located on other intracranial arteries. The tortuosity and curvature measures also depend on image quality and segmentation algorithms, which can introduce variability. Finally, we conducted a cross-sectional analysis of untreated aneurysms, and longitudinal data on aneurysm growth or rupture would be needed to validate these metrics as true prognostic markers. Future research should address these gaps.

Conclusions

Small ICA aneurysms occur preferentially on more tortuous vessels with a smaller parent-artery radius. These findings support the integration of 3D vessel geometry metrics into research of aneurysm risk stratification and treatment planning algorithms.

Disclosures

1. Institutional review board statement: This retrospective study utilised data from the medical records of patients hospitalised at the Department of Neurosurgery and Neurotraumatology, Jagiellonian University Medical College in Cracow, Poland (approval number: 1072.6120.348.2022), and it adhered to the principles outlined in the Declaration of Helsinki.
2. Assistance with the article: None.
3. Financial support and sponsorship: None.
4. Conflicts of interest: None.
5. AI use statement: During the preparation of this work, the authors used ChatGPT and Perplexity to perform language checks and corrections. After using this tool/service, the authors reviewed and edited the content as needed and took full responsibility for the content of the publication.

References

1. Sanchez S, Hickerson M, Patel RR, Ghazaleh D, Tarchand R, Paranjape GS, et al. Morphological characteristics of ruptured brain aneurysms: a systematic literature review and meta-analysis. Stroke Vasc Interv Neurol 2023; 3: e000707. DOI: 10.1161/SVIN.122.000707.
2. Wang GX, Zhang D, Wang ZP, Yang LQ, Yang H, Li W. Risk factors for ruptured intracranial aneurysms. Indian J Med Res 2018; 147: 51-57.
3. Rutledge C, Jonzzon S, Winkler EA, Raper D, Lawton MT, Abla AA. Small aneurysms with low PHASES scores account for a majority of subarachnoid hemorrhage cases. World Neurosurg 2020; 139: e580-e584. DOI: 10.1016/j.wneu.2020.04.074.
4. Froelich JJ, Neilson S, Peters-Wilke J, Dubey A, Thani N, Erasmus A, et al. Size and location of ruptured intracranial aneurysms: a 5-year clinical survey. World Neurosurg 2016; 91: 260-265.
5. Johnsen LH, Herder M, Vangberg T, Kloster R, Ingebrigtsen T, Isaksen JG, Mathiesen EB. Prevalence of unruptured intracranial aneurysms: impact of different definitions – the Tromsø Study. J Neurol Neurosurg Psychiatry 2022; 93: 902-907.
6. Bijlenga P, Gondar R, Schilling S, Morel S, Hirsch S, Cuony J, et al. PHASES score for the management of intracranial aneurysm. Stroke 2017; 48: 2105-2112.
7. Etminan N, Brown RD, Beseoglu K, Juvela S, Raymond J, Morita A, et al. The unruptured intracranial aneurysm treatment score. Neurology 2015; 85: 881-889.
8. Krzyżewski RM, Kliś KM, Kwinta BM, Stachura K, Popiela T, Gąsowski J. Association of arterial tortuosity with haemodynamic parameters – a computational fluid dynamics study. Brain Spine 2022; 2 (Suppl 2): 101414. DOI: 10.1016/j.bas.2022.101414.
9. Krzyżewski RM, Kliś KM, Kwinta BM, Łasocha B, Brzegowy P, Popiela TJ, Gąsowski J. Subarachnoid hemorrhage from ruptured internal carotid artery aneurysm: association with arterial tortuosity. World Neurosurg 2022; 166: e84-e92. DOI: 10.1016/j.wneu.2022.06.101.
10. Juchler N, Schilling S, Bijlenga P, Kurtcuoglu V, Hirsch S. Shape trumps size: image-based morphological analysis reveals that the 3D shape discriminates intracranial aneurysm disease status better than aneurysm size. Front Neurol 2022; 13: 809391. DOI: 10.3389/fneur.2022.809391.
11. Kim HJ, Song HN, Lee JE, Kim YC, Baek IY, Kim YS, et al. How cerebral vessel tortuosity affects development and recurrence of aneurysm: outer curvature versus bifurcation type. J Stroke 2021; 23: 213-222.
12. Kliś K, Krzyżewski R, Kwinta B, Stachura K, Gąsowski J. Tortuosity of the internal carotid artery and its clinical significance in the development of aneurysms. J Clin Med 2019; 8: 237. DOI: 10.3390/jcm8020237.
13. Piccinelli M, Veneziani A, Steinman DA, Remuzzi A, Antiga L. A framework for geometric analysis of vascular structures: application to cerebral aneurysms. IEEE Trans Med Imaging 2009; 28: 1141-1155.
14. Kliś KM, Wójtowicz D, Kwinta BM, Stachura K, Popiela TJ, Frączek MJ, et al. Association of arterial tortuosity with hemodynamic parameters – a computational Fluid Dynamics Study. World Neurosurg 2023; 180: e69-e76. DOI: 10.1016/j.wneu.2023.07.152.
15. Li R, Zhou P, Kao E, Zhu C, Mossa-Basha M, Wang Y. Unilateral cerebral arterial tortuosity: associated with aneurysm occurrence, but potentially inversely associated with aneurysm rupture. Eur J Radiol 2023; 165: 110941. DOI: 10.1016/j.ejrad.2023.110941.
16. Benemerito I, Ewbank F, Narracott A, Villa-Uriol MC, Narata AP, Patel U, et al. Computational fluid dynamics and shape analysis enhance aneurysm rupture risk stratification. Int J Comput Assist Radiol Surg 2025; 20: 31-41.